Chemical Geology 636 (2023) 121638

Contents lists available at ScienceDirect

Chemical Geology

journal homepage: www.elsevier.com/locate/chemgeo

Nitrogen uptake by methanotrophic consortia in deep-water gas hydrate-bearing sediments

Claudio Argentino [a,*], Cathrin Wittig [b,c], Jörn Peckmann [d], Giuliana Panieri [a]

[a] Department of Geosciences, UiT – The Arctic University of Norway, Tromsø, Norway
[b] Faculty of Sciences, Marine Biology Research Group, Ghent University, Ghent, Belgium
[c] Operational Directorate Natural Environment, Royal Belgian Institute of Natural Sciences, Brussels, Belgium
[d] Center for Earth System Research and Sustainability, Institute for Geology, Universität Hamburg, Hamburg, Germany

ARTICLE INFO

Editor: Hailiang Dong

Keywords:
Methane seep
Nitrogen uptake
Nitrogen cycle
Methane biogeochemistry
Barents Sea
Håkon Mosby Mud Volcano
Stable isotopes

ABSTRACT

Methane-consuming microbes inhabiting marine methane seeps have recently been found to have the capacity to assimilate inorganic nitrogen, suggesting a previously unaccounted role in the global nitrogen cycle. Despite ex-situ experimental observations, definitive evidence of this process under in-situ conditions remains elusive, hindering the complete understanding of the controlling factors and magnitude of this process. We present the isotopic variations of organic carbon $\delta^{13}C_{org}$ and total nitrogen $\delta^{15}N$ values in two sediment cores collected from the gas hydrate-bearing Håkon Mosby Mud Volcano, SW Barents Sea (72°N, ~1260 m water depth). We identified a stratigraphic interval containing methane-derived carbonates directly overlying a gas hydrate layer at 67 cm and typified by $\delta^{13}C_{org}$ and $\delta^{15}N$ as low as −42.0‰ and 1.2‰, respectively. Stable isotope mixing models confirm in-situ nitrogen uptake by methanotrophic consortia, contributing to up to 49.1 wt% of the local bulk sedimentary organic matter – a finding calling for reevaluation of the role of methane seeps in the oceanic nitrogen cycle.

1. Introduction

Microbial methane consumption in anoxic sediments plays a critical role in limiting ocean greenhouse gas fluxes into the atmosphere, which account for only 3–6% of today's total natural emissions (Weber et al., 2019). The biogeochemical process known as anaerobic oxidation of methane (AOM) occurs in the sediment of all continental margins and acts as an effective biofilter consuming approximately 90% of the upward migrating methane before entering the ocean (Reeburgh, 2007). AOM is performed by microbial consortia consisting of methanotrophic archaea (ANME) (Knittel et al., 2005) and sulfate-reducing bacteria (SRB) belonging to the Deltaproteobacteria (Orphan et al., 2001; Schreiber et al., 2010). This syntrophic consortium shares the energy yield deriving from the oxidation of methane to carbon dioxide coupled with the reduction of dissolved sulfate to sulfide via electron transfer (McGlynn et al., 2015; Wegener et al., 2015). In addition to the well-constrained carbon assimilation pathways in ANME-SRB consortia, metagenomic studies identified the presence of the nitrogenase genes (*nif*) responsible for nitrogen fixation in ANMEs (Dekas et al., 2009; Miyazaki et al., 2009; Orphan et al., 2009). The discovery of diazotrophy, the metabolic ability to fix dinitrogen into bioconvertible nitrogen species, associated with AOM was a significant breakthrough (Fulweiler, 2009), opening new research directions in deep-sea biogeochemistry, driven by the need to understand the distribution, abundance, and identity of nitrogen-fixing organisms in marine environments (Dekas et al., 2018; Dekas et al., 2016; Dekas et al., 2014; Dong et al., 2022; Metcalfe et al., 2021) and their unaccounted role in the global nitrogen cycle. In fact, current ocean models point to an unbalanced relationship between nitrogen sinks (i.e. denitrification) and sources (i.e. nitrogen fixation; Codispoti, 2007; Hutchins and Capone, 2022; Mahaffey, 2005). In addition, methanotrophic consortia can perform anabolic ammonium (NH_4^+) assimilation, as demonstrated by incubation studies and stable isotope labelling experiments (Dekas et al., 2018; Dekas et al., 2014; Dekas et al., 2009; Orphan et al., 2009). Diazotrophy is assumed to be a metabolic strategy to overcome nitrogen limitation when the other bioavailable nitrogen forms (NH_4^+, NO_3^-) in pore waters are depleted, but it is still unclear what environmental conditions influence this process since some authors reported peaks in nitrogen fixation rates in coastal marine sediments at high ammonium concentration (> 1 mM)(Bertics et al., 2010). In methane seep

* Corresponding author.
E-mail address: claudio.argentino@uit.no (C. Argentino).

https://doi.org/10.1016/j.chemgeo.2023.121638
Received 28 April 2023; Received in revised form 3 July 2023; Accepted 18 July 2023
Available online 19 July 2023

sediments, ammonium seems inhibiting ANME diazotrophy at concentrations ≥25 μM (Dekas et al., 2018), but localized nitrogen fixation can occur in ammonium-depleted microniches in the sediment or within large ANME-SRB aggregates characterized by size-induced micro-gradients with lower ammonium concentration near the core of the consortia (Dekas et al., 2014; Metcalfe et al., 2021; Orphan et al., 2009). Although the potential for inorganic nitrogen assimilation has been experimentally validated ex-situ for both ANME (Dekas et al., 2014; Dekas et al., 2009; Orphan et al., 2009) and SRB (Metcalfe et al., 2021), direct evidence from marine seep sediments is scarce, limiting our ability to assess the role of AOM in the global nitrogen cycle. As methane seeps and gas hydrates are widespread along continental margins (Piñero et al., 2013), verifying the occurrence of AOM-driven nitrogen uptake in those environments is critical to assess the distribution and magnitude of methanotrophy-related nitrogen cycling. Such knowledge may help solve current discrepancies in the oceanic nitrogen budget (Dekas et al., 2014).

The isotopic fractionation associated with marine nitrogen fixation leads to $\delta^{15}N$ values approximately 1‰ to 6‰ lower than the values of the dissolved nitrogen substrate (Zhang et al., 2014), typically resulting in biomass with $\delta^{15}N$ values from −2 to 0‰ (Altabet, 2007; Dekas et al., 2018; Montoya, 2008). Ammonium assimilation can produce an apparent fractionation of up to −27‰ (Hoch et al., 1992), leading to similarly low $\delta^{15}N$ values of biomass (Yamanaka et al., 2015). Therefore, discriminating between the two processes (diazotrophy and ammonium assimilation), is not possible with an isotopic approach alone and requires targeted microbiological investigations. However, the isotopic signature of the uptake of inorganic nitrogen is characterized by lower values than the average $\delta^{15}N$ composition of sedimentary organic matter ranging from 3 to 7‰ (Emerson and Hedges, 1988; Meyers, 1994), composed of a mix of marine and terrestrial sources, representing a potential for its use as a proxy in the sedimentary record. To date only little evidence for the existence of AOM-related nitrogen uptake in marine sediment exists, including low $\delta^{15}N$ values of bulk organic matter in sediments from the Gulf of Mexico (Joye et al., 2004) and negative excursions of $\delta^{15}N$ values up to −5‰ at seeps in the South China Sea compared to non-seep sediment (Hu et al., 2020). In those studies, the hypothesized relationship between AOM and diazotrophy was based on concomitantly decreasing $\delta^{13}C_{org}$ values (Joye et al., 2004) and other sedimentary proxies for AOM at the SMTZ (Hu et al., 2020). Still, carbon isotopic values of organic matter were not mirroring trends of values of marine and terrestrial sources or were not reported.

Here, we present first combined $\delta^{13}C$ and $\delta^{15}N$ isotopic evidence of the uptake of inorganic nitrogen by AOM consortia, studying sediments collected from the gas-hydrate bearing Håkon Mosby Mud Volcano (HMMV), SW Barents Sea (Fig. 1a). Since nitrogen assimilation by ANME-SRB appeared to be dependent on high methane levels in laboratory experiments (Dekas et al., 2018; Dekas et al., 2014; Dekas et al., 2009), HMMV represents an ideal area to investigate this process in the environment. We characterized the sediment biogeochemistry of two gravity cores (Figs. 1b, c) collected during expedition CAGE20–3. We interpret pore water sulfate concentrations and profiles of dissolved inorganic carbon isotopes ($\delta^{13}C_{DIC}$), methane concentration in the sediment and its isotopic composition ($\delta^{13}C_{CH4}$), molecular and isotopic composition of bulk decarbonated sediment (TOC, $\delta^{13}C$, TN, $\delta^{15}N$), and downcore X-ray fluorescence Ca and Ba concentration profiles. This study demonstrates the occurrence of AOM-driven uptake of inorganic nitrogen in gas hydrate-bearing sediments, encouraging further investigations in similar modern settings and the rock record.

2. Geological setting

The Håkon Mosby Mud Volcano is located at ~1260 m water depth (Fig. 1a) on the SW Barents Sea slope (Fig. 1a). The volcano is approximately 1.4 km in diameter and covers an area of 1.2 square km (Figs. b, c), with a ~ 15 m high relief above the seafloor. The stratigraphy in this area is characterized by a sedimentary succession approximately 6 km in thickness, overlying oceanic crust (Faleide et al., 1996). The formation of HMMV is attributed to the accumulation of overpressure in the gas-rich hemipelagic glacial units due to successive sliding in the upper slope during the Cenozoic (Perez-Garcia et al., 2009). The occurrence of the Bear Island Slide at ~330 ka BP led to a sudden decrease in overburden and consequent sediment load further downslope. This event triggered the lateral upslope migration of gas-rich fluids along the Bear

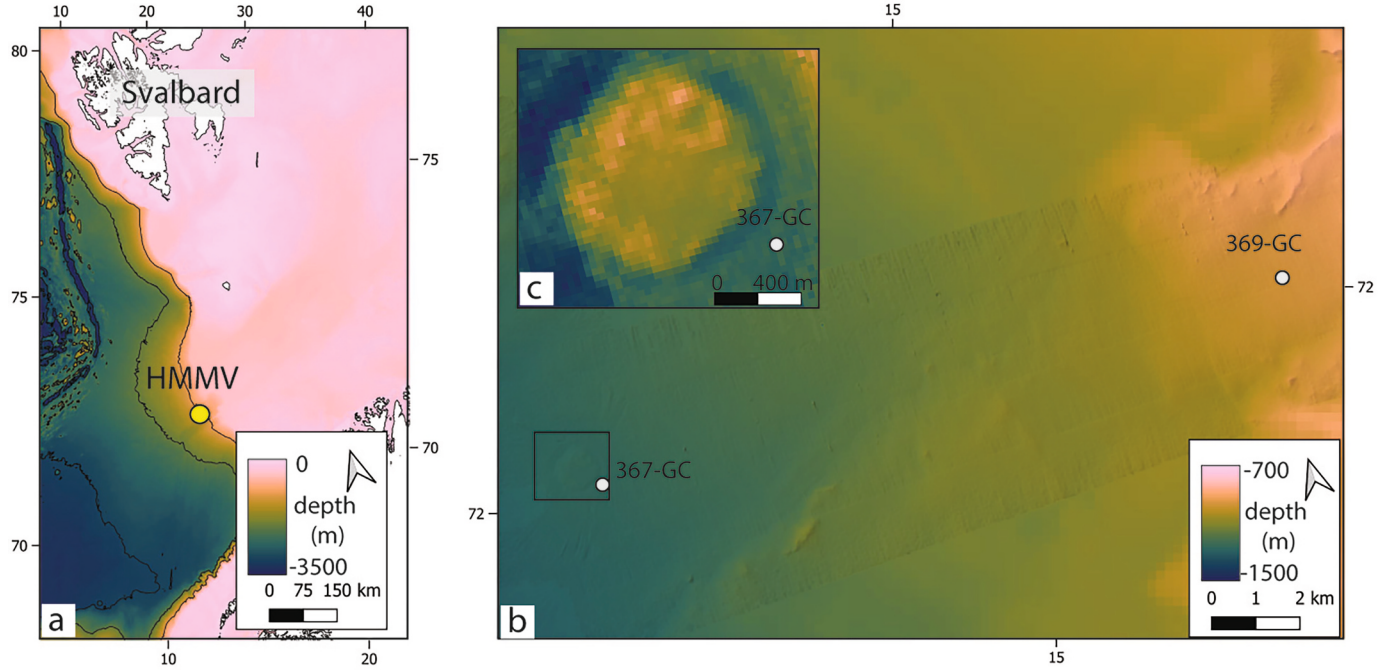

Fig. 1. Location and bathymetry of the study area and investigated sediment cores. (a) The Håkon Mosby Mud Volcano is located on the slope of the SW Barents Sea. (b) The gravity cores were collected from the mud volcano at ~1260 m water depth (367-GC) and from a reference site at 965 m (369-GC). (c) Close-up view of the mud volcano. The color scale is accessible to people with color vision deficiencies (Crameri et al., 2020).

Island Slide scar weakness zone with consequent mud remobilization (Perez-Garcia et al., 2009). High resolution 2D Seismic and sediment sub-bottom profiles revealed a narrow conduit rooting in at least 3 km depth in the Late Pliocene sediments, constituting the main pathway for focused upward fluid and mud flow (Perez-Garcia et al., 2009). A shallow mud chamber has been discovered at ~300 m depth, directly above the Bear Island Slide scar and is linked to the surface via a narrow vertical conduit (Perez-Garcia et al., 2009). The main hydrocarbon reservoir is located in the pre-glacial biosiliceous oozes deposited in the early-mid Cenozoic (Hjelstuen et al., 1999). The HMMV hosts abundant type I (methane-rich) gas hydrates in the shallow subsurface (Pape et al., 2011), and the seafloor is inhabited by widespread chemosynthesis-based communities of *Beggiatoa* mats and frenulate siboglinid tubeworms (Figs. 2a, b)(Bünz and Panieri, 2022; Niemann et al., 2006), whose distribution is primarily controlled by methane gradients in the sediment. In this study we focus on two gravity cores from the HMMV area. One core contained gas hydrates (367-GC), which rapidly dissolved onboard (Fig. 2c), while a reference core was collected 16 km away from HMMV (Fig. 1b) and is used as a reference (369-GC).

3. Methods

3.1. Sediment and pore fluid samplings

Sediment cores 367-GC and 369-GC were collected in 2020 during the expedition CAGE20–3 with R/V *Helmer Hanssen* using a 6-m long gravity corer. The cores were cut onboard into 1 m sections and immediately sampled for pore water and headspace gas. Pore water was extracted using rhizon samplers and 10 mL sterile syringes. All pore water samples were split into two aliquots for sulfate and dissolved inorganic carbon analyses. DIC samples were fixed with 10 μL of $HgCl_2$ saturated solution. Sulfate samples were stored at −20 °C, while DIC samples were kept at 4 °C in the dark. A bulk sediment sample for headspace gas analysis was collected from the bottom of core 367-GC using a cut-off syringe. The sample was transferred into a glass vial prepared with 5 mL of 1 M NaOH to stop microbial activity, sealed with

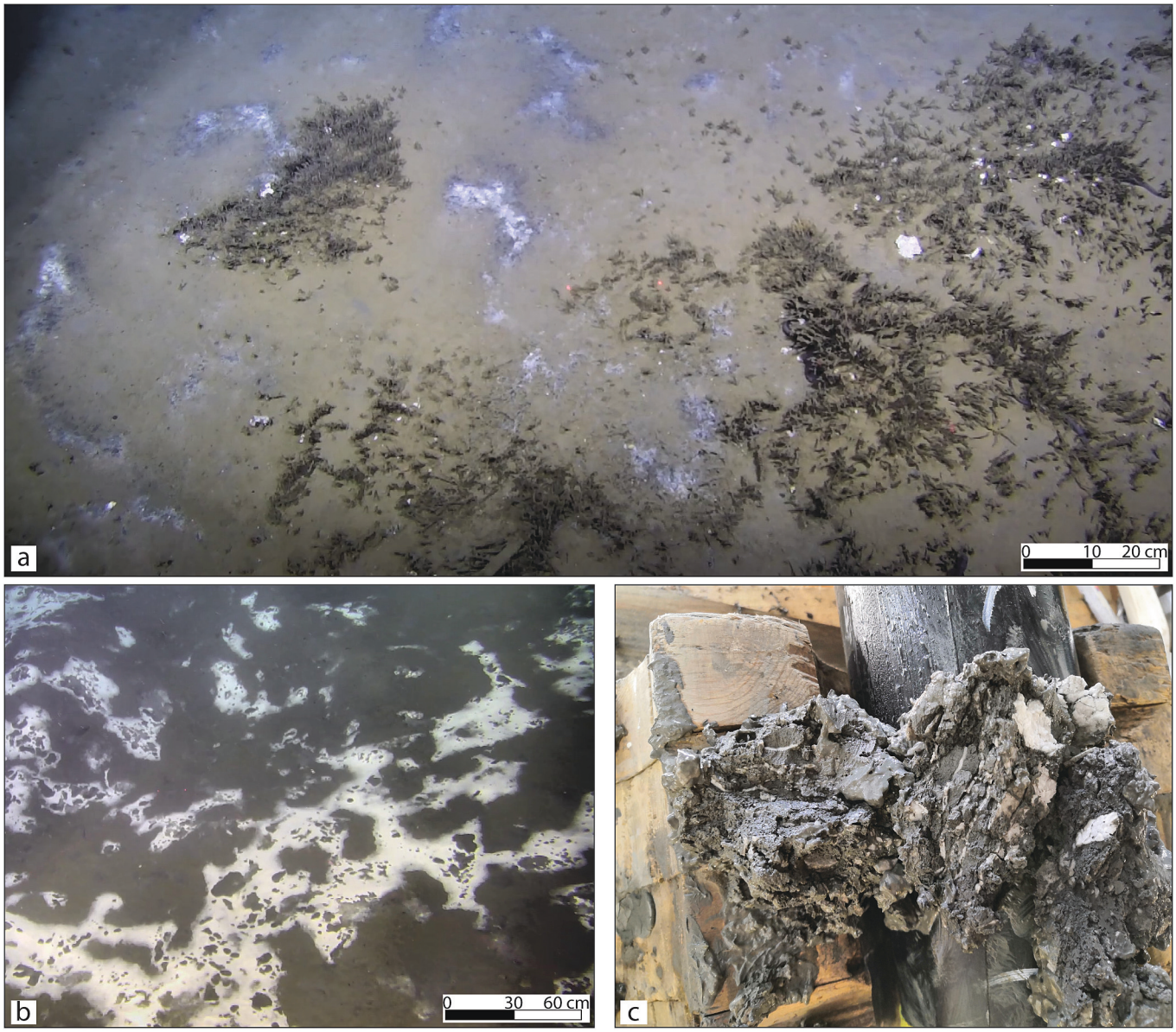

Fig. 2. Seafloor imagery and gas hydrates at Håkon Mosby Mud Volcano. (a) HMMV is an active seepage area with widespread seafloor chemosynthesis-based communities, including *Beggiatoa* mats and frenulate siboglinid tubeworms. Imagery collected during expedition CAGE21–1 (Bünz and Panieri, 2022). (b) Large bacterial mats from HMMV. (c) Gas hydrates at the bottom of gravity core 367-GC observed during research expedition CAGE20–3.

a rubber septum and aluminum crimp cap, shaken and then stored upside-down at 4 °C.

3.2. Sediment logging

High-resolution (1 mm) magnetic susceptibility and porosity measurements were conducted on whole-core sections of 367-GC and 369-GC using a GEOTEK Multi Sensor Core Logger (MSCL) hosted at the Geology Laboratory (UiT). X-Ray fluorescence core logging was conducted on cores 367-GC and 369-GC using an Avaatech XRF Core Scanner at 1 cm steps. Datasets were acquired in multiple runs at different currents, voltages and filters: 10 kV, 1 mA, no filter; 30 kV, 2 mA, Pd-thick filter; 50 kV, 2 mA, Cu-filter. The measuring time varied for every run:10 s (10 kV) and 20 s (30 kV and 50 kV). For this study, we report the calcium and barium counts normalized to titanium to correct for the matrix effect and transformed to log ratios to enable peak amplitude comparisons. Ln(Ca/Ti) and ln(Ba/Ti) profiles were smoothed by applying an unweighted sliding-average algorithm to suppress false peaks caused by random noise.

3.3. Sediment carbon-nitrogen systematics ($\delta^{13}C_{org}$, $\delta^{15}N_d$, C/N) and methane-derived carbonate isotope geochemistry ($\delta^{13}C$ and $\delta^{18}O$)

Sediment samples for carbon and nitrogen geochemistry were collected from cores split into half (every cm from 367-GC and every 5 cm from 369-GC). Approximately 0.3 g of dry sediments were weighed in 10 mL Eppendorf tubes and treated with 5 ml 6 N HCl to remove the carbonate component. Samples were rinsed five times with distilled water and let to dry out in the oven at 50 °C. Analyses were conducted at the Stable Isotope Laboratory-SIL at the Centre for Arctic Gas Hydrate, Environment and Climate (CAGE) located at the UiT-The Arctic University of Norway, in Tromsø, Norway, using a Thermo-Fisher MAT253 Isotope Ratio Mass Spectrometer (IRMS) coupled to a Flash HT Plus Elemental Analyzer. The $\delta^{13}C$ and $\delta^{15}N$ values of decarbonated material were determined by normalization to international standards, Vienna Pee Dee Belemnite, VPDB ($\delta^{13}C$) and Air-N_2 ($\delta^{15}N$), by three in-house standards. The analysis of duplicate samples throughout the session yielded an average repeatability (1SD; $N = 6$) for TOC, TN, $\delta^{13}C$ and $\delta^{15}N$ of 0.1 ± 0.3%, 0.01 ± 0.03%, 0.4 ± 1.7‰, and 0.4 ± 1.1‰, respectively. The C/N atomic ratio was calculated using the atomic mass weighted ratio of TOC and TN as C/N = (TOC/12.011)/(TN/14.007). The proportions of marine and terrestrial organic matter and AOM-related biomass in bulk sedimentary organic matter were calculated using the ISOCONC1_01.xls is Microsoft Excel 2000™ spreadsheet openly available from the United States Environmental Protection Agency (EPA). Methane-derived authigenic carbonates were hand-picked from dry sediment samples, and their carbon and oxygen isotopic composition was determined on a MAT 253 IRMS. Data are reported in ‰ notation relative to VPDB. The analytical error was better than 0.1‰ (1SD) for both carbon and oxygen.

3.4. Pore fluid analyses

The carbon isotopic composition of dissolved inorganic carbon (DIC) in cores 367-GC and 369-GC was measured at the Stable Isotope Laboratory-SIL (UiT) using a Thermo Scientific MAT253 IRMS (Thermo Fischer Scientific, U.S.A.) coupled to a Gasbench II. Three in-house calcite standards were used for normalization to VPDB and provided analytical precision of 0.1‰ (1SD; $N = 5$). Sulfate concentration was measured via ion chromatography at TosLab AS in Tromsø, Norway, following the NS-EN ISO 10304-1 method. Gas in the sediment was measured in headspace samples. We collected 5 ml of bulk sediment from different stratigraphic intervals and the material was transferred into 20 ml serum vials containing and 5 ml of 1 M NaOH. The vials were sealed with a septum and an aluminum crimp cap and stored at 4 °C. Methane concentration was measured using a ThermoScientific Trace 1310 gas chromatograph at the Stable Isotope Laboratory-SIL (UiT). Methane isotope composition in the headspace gas sample was separated on a Restek MXT Molsieve 5 Å gas chromatography column and measured using a Nu Horizon (Nu Instruments Ltd., UK) at IFE, Institute for Energy Technology (Oslo, Norway). Calibration was done with in-house standards calibrated with the international standards USGS NGS-2 and USGS NGS-3. Precision on $\delta^{13}C$ of methane was estimated as 0.5‰ VPDB (1SD).

4. Results and discussion

4.1. Sediment biogeochemistry

The sediment cores collected from the HMMV (367-GC) and background area (369-GC) show high variability in the magnitude of subsurface fluxes and biogeochemical processes. In marine sediments, AOM occurs in a redox interval referred to as the sulfate-methane transition zone (SMTZ), situated at the interception of methane and sulfate concentration profiles and located at various depths beneath the seafloor ranging from 0.5 m in shelf settings to >150 m in abyssal regions (Egger et al., 2018). In seepage-impacted sediments, the SMTZ can be as shallow as a few cm (Argentino et al., 2022; Argentino et al., 2021; Fischer et al., 2012; Lee et al., 2019), and AOM rates are several orders of magnitude higher than in background sediments (Lee et al., 2019; Marlow et al., 2014). Reference core 369-GC does not show evidence of a present-day SMTZ down to a depth of 350 cm (Fig. 3a). Sulfate concentrations and $\delta^{13}C_{DIC}$ values decrease down-core with minimum values of 14 mM and − 16.2‰, respectively. Methane has been found in trace amounts, ranging from 1.3 to 5.1 μM. Such patterns are typical of the sulfate reduction zone of marine sediments, where organic matter decomposition coupled with sulfate reduction is the dominant biogeochemical process controlling pore water sulfate and DIC gradients. The XRF dataset defines three lithological units separated by sharp Ba and Ca gradients (Fig. 3a) and associated with different porosity and magnetic susceptibility (Supplementary Fig. 1). There is no sedimentological indication for mass flow deposits in the X-ray logs (Fig. 3a). Therefore, these units reflect in-situ deposition, and their geochemical composition is related to changes in productivity. Overall, these observations indicate that core 369-GC is not affected by methane oxidation and can be used as a reference for the hydrate-bearing core.

Gravity core 367-GC intercepted a gas hydrate-rich layer at ca. 67 cm below the seafloor (Fig. 2c). The sediment becomes stiffer and drier close to the top of the hydrate layer, interpreted to reflect absorption of water molecules during gas hydrate formation and associated with a progressive decrease in porosity (Supplementary Fig. 1). A headspace gas sample collected at the base of the core yielded a $\delta^{13}C_{CH4}$ value of −52.3‰, close to the values of around −60‰ previously reported from HMMV (Lein et al., 1999; Pape et al., 2011). Methane concentration at 30 cm depth is 2.0 mM, three orders of magnitude higher than in the reference core. The sulfate profile of core 367-GC exhibits a concave-up shape (Fig. 3b) suggesting non-steady state conditions induced by an increase in methane flux (Schulz, 2006). Sulfate is fully consumed at around 50 cm depth, marking the position of the modern SMTZ. The carbon isotopic composition of DIC reaches a minimum $\delta^{13}C$ value of −31.2‰ at the same depth (Fig. 3b, Supplementary Table 1), indicating a contribution from methane-derived carbon released by AOM into the pore water. Higher $\delta^{13}C_{DIC}$ values below the SMTZ cannot be explained by isotopic fractionation related to hydrate formation, since that process only involves the hydrogen isotopes leaving the carbon isotopic composition of hydrate-bound molecules and residual gas unaltered (Hachikubo et al., 2007). Therefore, we ascribe the observed trend as due to the presence of residual ^{13}C-enriched DIC related to methanogenesis (Whiticar, 1999). Two concretions of authigenic carbonate from the 60–61 cm and 64–65 cm intervals (Fig. 3b) yielded $\delta^{13}C$ values of −31.8‰ and − 31.6‰ and $\delta^{18}O$ values of 6.1‰ and 5.8‰, respectively, which are typical of methane-derived authigenic carbonates (MDAC)

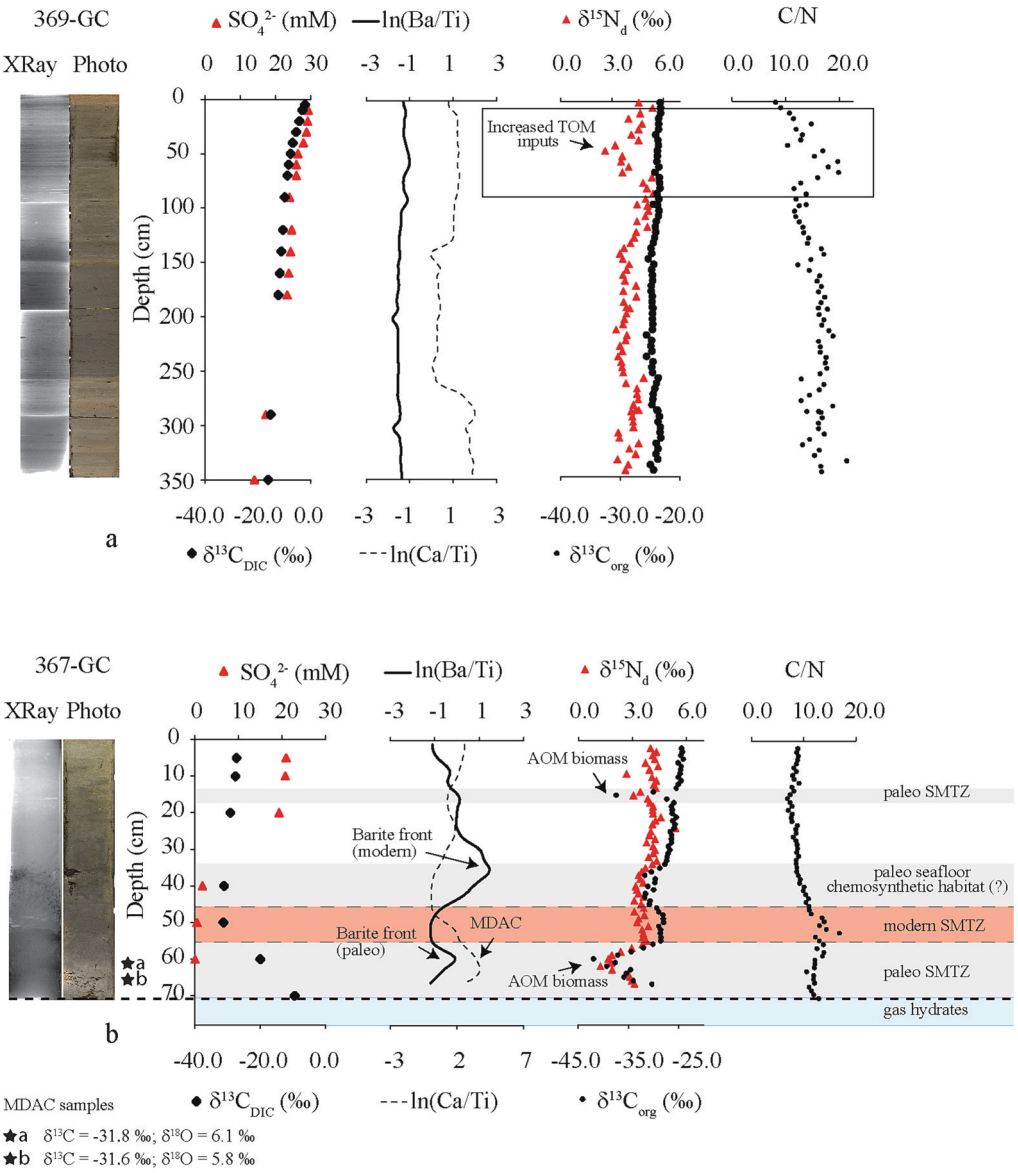

Fig. 3. Sediment and pore water geochemistry of sediment cores. (a) Reference core 369-GC shows a low sulfate concentration gradient and $\delta^{13}C_{DIC}$ profile, indicating no current AOM activity. Nitrogen isotopic composition in decarbonated sediment ($\delta^{15}N_d$) and C/N ratios reflect the influence of terrestrial input (TOM = terrestrial organic matter) corresponding to a laminated stratigraphic unit apparent at the top of the core in the X-ray images. (b) The gas-hydrate-bearing core 367-GC hosts an SMTZ at ca. 50 cm depth and paleo-SMTZs marked by abrupt declines in $\delta^{13}C_{org}$ and $\delta^{15}N_d$ values in the intervals 14–16 cm and 55–67 cm, the latter being associated with methane-derived carbonates. The stratigraphic interval 34–47 cm is typified by low carbon isotopic values in bioturbated sediment, possibly linked to a paleo-seafloor colonized by chemosynthesis-based fauna as observed at the modern seabed.

incorporating variable amounts of ^{13}C-depleted carbon released by AOM. The carbon and oxygen values are respectively higher and lower than the values of methane-derived carbonates reported in a previous study from Håkon Mosby Mud Volcano, $-29.6‰ < \delta^{13}C < -28.4‰$ and $4.3‰ < \delta^{18}O < 5.4‰$ (Milkov et al., 2004), possibly reflecting the proximity to hydrate in core 367-GC. The data presented in Fig. 3b agree with MDAC formation at a paleo-SMTZ. The XRF peaks in calcium at 61 cm depth are therefore ascribed to the presence of MDACs. Interestingly, the isotopic composition of carbonate minerals is close to the measured $\delta^{13}C_{DIC}$ value at 50 cm depth. Thus the carbonates probably formed before the upward shift of the SMTZ started a few tens to hundreds of years ago (Kasten et al., 2003). The current SMTZ coincides with a small bulge in ln(Ca/Ti), coinciding with ongoing MDAC formation. The modeled oxygen isotope composition of carbonate forming in equilibrium with modern bottom waters (~0‰ SMOW; BWT = −1 °C)(Lein et al., 1999; Milkov et al., 2004) is 4.2‰ for aragonite (Kim et al., 2007) and 5.2‰ for high-Mg calcite (Friedman and O'Neil, 1986). The $\delta^{18}O$ values of the studied carbonates are higher than the calculated theoretical values, indicating a significant contribution of isotopically-heavy water from gas hydrate dissociation (Davidson et al., 1983). XRF data reveal barium enrichments with peaks at around 35 cm and 60 cm depth (Fig. 2b). Barium is common in seepage-affected sediments, forming diagenetic fronts at the top of the SMTZ (Riedinger et al., 2006). For core 367-GC, the prominent peak at 35 cm is interpreted to reflect the current SMTZ, whereas an increase of contents within the MDAC interval represents a remnant of the paleo-SMTZ.

4.2. Evidence of nitrogen uptake by AOM consortia

The carbon-nitrogen systematics (C/N ratios, $\delta^{13}C_{org}$, $\delta^{15}N_d$) of sediment cores was used to characterize the background sedimentary organic matter composition (marine vs terrestrial) and to identify post-depositional diagenetic signals related to AOM-derived microbial biomass. Marine-derived organic matter is typically characterized by $\delta^{13}C$ values between −23‰ and − 16‰ (Emerson and Hedges, 1988; Meyers, 1994), $\delta^{15}N$ values as high as 7‰ (Wada, 1980), and C/N ratios between 4 and 10 (Meyers, 1994). In contrast, terrestrial organic matter is typified by lower $\delta^{13}C$ values ranging between −28‰ and − 26‰ (Emerson and Hedges, 1988; Meyers, 1994), lower $\delta^{15}N$ values (Kienast et al., 2005), and C/N ratios higher than 20 (Emerson and Hedges, 1988; Meyers, 1994). The accumulation of AOM-derived biomass in marine sediments depends on the overall methane flux and sulfate availability,

as well as the stability of the SMTZ at a particular depth (Hinrichs et al., 2000). Therefore, significant shifts in bulk $\delta^{13}C_{org}$ of marine sediments linked to methanotrophic biomass are expected in sediment samples collected from modern or past SMTZs in methane seepage areas. Extreme ^{13}C depletion with $\delta^{13}C_{org}$ as low as ca. -60‰ has been discovered in the geological record of the early Earth (Eigenbrode and Freeman, 2006) and attributed to globally widespread methanotrophy, indicating the potential use of this parameter as a proxy for AOM in sediments as old as 2 Ga. In modern MDAC, bulk $\delta^{13}C_{org}$ values are as low as −81‰ (Feng et al., 2021), consistent with a total organic carbon composition dominated by methanotrophic biomass. On the other hand, the univocal recognition of an AOM-related $\delta^{13}C_{org}$ signal in modern bulk sediment samples is scarcely reported in the literature, as it is generally associated with small shifts of 1–3‰ (Argentino et al., 2021; Lee et al., 2018; Miao et al., 2022) or it is masked by isotopic signals of other carbon sources (Li et al., 2022).

Here, we measured $\delta^{13}C_{org}$ values as negative as −42.0‰ (60 cm) in sediments directly overlying the gas hydrate-bearing interval (Fig. 3b, Supplementary Table 2). Reference core 369-GC shows a relatively constant downcore $\delta^{13}C_{org}$ composition with a mean value of −24.2 ± 0.6‰ (1SD; $n = 73$)(Fig. 3a, Supplementary Table 2), indicating the predominance of marine and terrestrial sources. The low $\delta^{13}C_{org}$ values measured in the sediment layer containing MDAC cannot be produced by a mixture of marine and terrestrial organic matter but only by considering an AOM-related contribution (Fig. 4a). We confidently interpret this $^{13}C_{org}$-depleted interval at 55–67 cm as related to high contents of methanotrophic biomass. The same value was measured in a short (20 cm) sediment core from the oxygen minimum zone off Pakistan (Yoshinaga et al., 2015) and ascribed to AOM-associated biomass based on total lipid extract and DNA analyses. In core 367, the gas hydrate layer favored protracted and intense sulfate-driven AOM in the overlying SMTZ, leading to the accumulation of high amounts of ^{13}C-depleted biomass in the sediment (Elvert et al., 2005). The generation of this remarkable isotopic depletion in the sediment was likely facilitated by low sedimentation rates, which ultimately control the period of time during which AOM activity takes place in a certain depth interval. The negative excursion in the carbon isotope profile of core 367-GC at 14–16 cm depth ($\delta^{13}C_{org} = -37.5$‰) is also consistent with AOM and a shallow paleo-SMTZ linked to the past hydrate dynamics. A $\delta^{13}C_{org}$ value of −32.3‰ has been found in gas hydrate-bearing sediments at Bullseye vent (SMTZ depth < 1 m), offshore Vancouver Island, Canada (Pohlman et al., 2013), whereas only a 1‰ drop and relatively high $\delta^{13}C$ value (−24.4‰), was measured at a deeper gas hydrate-associated SMTZ at 170 m below the seafloor (Xiong et al., 2020). The variability in $\delta^{13}C_{org}$ values in gas hydrate-bearing sediments in this study, therefore, seems to be controlled by the proximity of the SMTZ to the gas hydrate source, methane fluxes and longevity of the SMTZ at a certain depth, with values increasing with distance from hydrate. The sediment interval at 34–47 cm depth also shows depleted isotopic signatures ($\delta^{13}C_{org}$ as negative as −31.8‰) compared to adjacent sediment intervals and the background sediment of core 369-GC (Fig. 3). The negative excursion at this depth is less well-defined than the sharp peaks observed at 15 cm and 60 cm but is still easily recognizable in the overall constant downward trend. The 34–47 cm depth interval is bioturbated (Fig. 3b). Microbial mats and tubeworm habitats are widespread at Håkon Mosby Mud Volcano today (Figs. 2a, b)(Bünz and Panieri, 2022); faunal distribution reflects the dynamic energy fluxes related to subsurface AOM. The observed bioturbation was probably created by seep fauna inhabiting a paleo-seafloor and fixing methane-derived carbon.

The nitrogen isotopic composition of total nitrogen was measured on decarbonated material (TN_d), and it is hereafter assumed to reflect organic nitrogen based on the close-to-zero-intercept of TN_d versus total organic carbon (TOC) (Supplementary Fig. 2). This assumption let us consider bulk sediment TN_d values as mixtures of different organic sources. In reference core 369-GC, the nitrogen isotope profile displays a negative peak centered at 46 cm depth, accompanied by an opposing trend in the C/N atomic ratio (Fig. 3a). This interval corresponds to a laminated lithological unit consisting of fine-grained turbidites, explaining the observed geochemical patterns caused by enhanced terrestrial input of organic matter with lower $\delta^{13}C$ and $\delta^{15}N$ values and low nitrogen contents (Meyers, 1994). Unlike the reference core, the nitrogen isotope composition shows remarkable downcore variation in the gas hydrate-bearing core 367-GC, with $\delta^{15}N$ values between 1.2‰ and 5.2‰. The downcore $\delta^{15}N$ profile matches the $\delta^{13}C_{org}$ profile (Fig. 3b). Methanotrophic consortia are known to have the capability of fixing nitrogen and assimilate ammonium, which leads to ^{13}C- and ^{15}N-

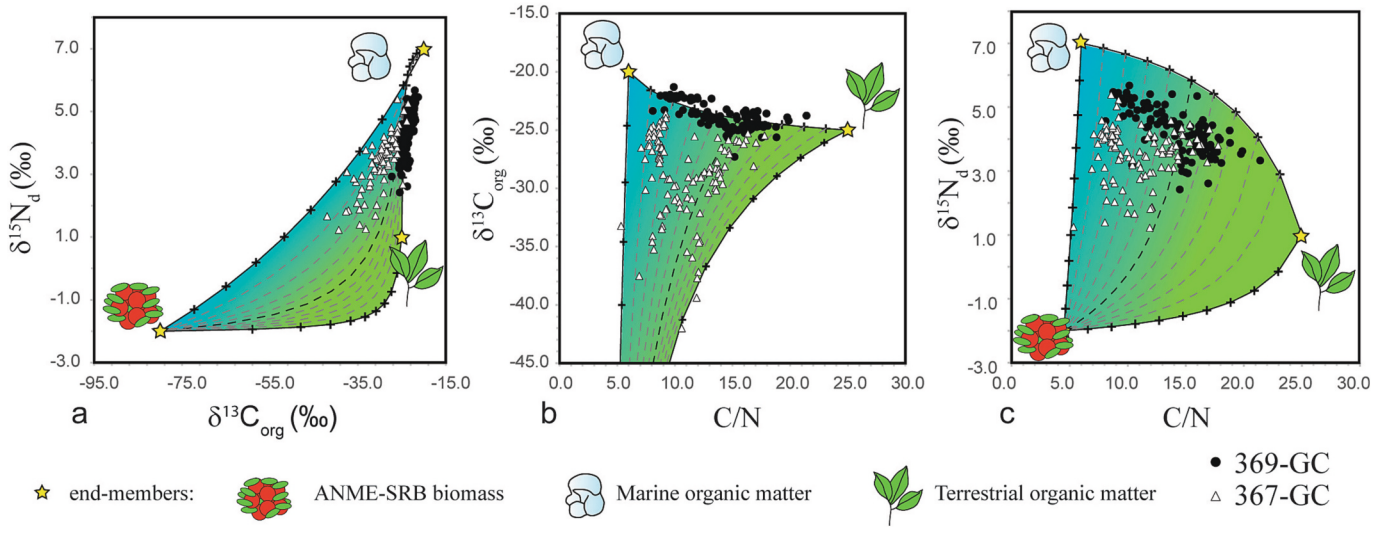

Fig. 4. Concentration-weighed stable isotope mixing models to distinguish the contribution of AOM-derived biomass (ANME-SRB) and bulk sedimentary organic matter. The mixing area (colored) within which the mixed samples plot is defined by the binary mixing lines between the two adjacent end-members. Crosses indicate 10% mixing increments. The dashed lines indicate MOM-TOM mixing proportions with 10% increments, and the bold line is 50% MOM - 50% TOM. (a) $\delta^{15}N_d$ vs $\delta^{13}C_{org}$ diagram showing that the reference core samples (369-GC) fall on the MOM-TOM mixing line, whereas the samples of the gas hydrate-bearing core (367-GC) follow the mixing trends defined by variable contributions of ANME-SRB biomass. (b) $\delta^{13}C_{org}$ vs C/N plot illustrating the carbon isotopic difference between 367-GC samples (values as negative as −42.0‰) and 369-GC samples (on the MOM-TOM mixing line). (c) $\delta^{15}N_d$ vs C/N diagram displaying lower isotopic values for the 367-GC core samples.

depleted biomass (Dekas et al., 2018; Dekas et al., 2014; Dekas et al., 2009; Orphan et al., 2009), and prominent negative $\delta^{15}N_d$ excursions were observed within the sulfate-methane transition in the South China Sea (Hu et al., 2020), putting forward the idea of an isotopic fingerprint of nitrogen uptake by ANME. Marine nitrogen uptake from diazotrophy is associated with modest isotopic fractionation leading to $\delta^{15}N$ values of organic matter of approximately −2 to 0‰ (Altabet, 2007; Montoya, 2008), and ammonium assimilation can produce similarly low bulk $\delta^{15}N$ values (Yamanaka et al., 2015). The isotopic signature of microbial nitrogen uptake in the sediment can be diluted by terrestrial inputs (Emerson and Hedges, 1988; Meyers, 1997; Wada, 1980), but the lack of an inverse correlation with C/N ratios in core 367-GC leads us to exclude that terrestrial sources are generating the observed nitrogen isotopic values. Therefore, the strict association of low $\delta^{15}N$ values with $\delta^{13}C$ values lower than −35‰ indicates that this isotopically-light nitrogen signal is related to the presence of biomass of methanotrophic consortia.

We estimated the contribution of AOM to the bulk sedimentary C-N composition by developing concentration-weighed stable isotope mixing models for $\delta^{15}N_d$ vs $\delta^{13}C_{org}$ (Fig. 4a), $\delta^{13}C_{org}$ vs C/N ratio (Fig. 4b), and $\delta^{15}N_d$ vs C/N ratio (Fig. 4c). We generated a three end-member scenario including marine, terrestrial, and AOM-related biomass as the dominant organic fractions in the sediment. We are aware that diverse nitrogen fixation communities not relying on sulfate-dependent anaerobic oxidation of methane might be present, but at seeps methanotrophic nitrogen fixers are predominant (Dong et al., 2022), and can make up as many as 94% of the total cells in the sediment (Boetius et al., 2000; Knittel et al., 2005). The selection of end-member values of $\delta^{13}C_{org}$, $\delta^{15}N_d$, and C/N for marine and terrestrial organic matter took advantage of published datasets for surface sediments of the Barents Sea (Knies et al., 2007; Knies and Martinez, 2009) and was slightly adjusted to fit the composition of the reference core 369-GC (Supplementary Fig. 3): marine organic matter $\delta^{13}C_{org} = -20‰$, $\delta^{15}N_d = 7‰$, $C/N = 6$; terrestrial organic matter $\delta^{13}C_{org} = -25‰$, $\delta^{15}N_d = 1‰$, $C/N = 25$. The $\delta^{13}C$ composition of ANME-SRB consortia is heterogeneous as they can incorporate various proportions of methane-derived carbon leading to bulk $\delta^{13}C_{org}$ values ~$\delta^{13}C_{DIC}$ to over 30 ‰ lower than the values of methane (House et al., 2009). We decided to adopt a $\delta^{13}C_{org}$ value of −80‰, approximating the lowest value measured in methane-derived carbonates from the Gulf of Mexico and the South China Sea (Feng et al., 2021) and compatible with the methane composition measured in core 367-GC. Although this assumption might not reflect the real end-member composition at this site, it does not affect the qualitative interpretation of the models. An end-member isotopic value higher or lower than the one used for our mixing models would lead to larger or smaller ANME-SRB contributions, respectively. Regarding the $\delta^{15}N_d$ composition of the ANME-SRB end-member, we selected a value of −2% as we found that more negative end-member values would fail to describe the variability in our datasets (the lowest values of the samples would plot off the diagram). Such value agrees with the range of values reported by Montoya (2008) for diazatrophy. We assumed an average microbial C/N value of 4.5 (Madigan et al., 2017). The preferential removal of nitrogen-rich compounds during early diagenesis can alter the elemental and isotopic composition of sedimentary organic matter, toward higher C/N and lower $\delta^{13}C_{org}$ and $\delta^{15}N$ (Altabet, 2005; Lehmann, 2002). Our models are not affected by post-depositional remineralization processes as the two investigated cores do not show such common patterns of variations.

On the $\delta^{15}N_d$ vs $\delta^{13}C_{org}$ plot, reference core samples fall on the mixing line of marine (MOM) and terrestrial (TOM) end-member organic matter, indicating negligible AOM influence (Fig. 4a). Samples from core 367-GC plot away from the MOM-TOM mixing line, reflecting variable mixing of MOM-TOM and AOM-derived biomass (ANME-SRB). Specifically, the $\delta^{15}N_d$ and $\delta^{13}C_{org}$ composition of most samples can be explained by admixture of 0–50% TOM, 50–100% MOM, and 0–50% ANME-SRB biomass. The contribution of ANME-SRB biomass is also evident from the $\delta^{13}C_{org}$ vs C/N and $\delta^{15}N_d$ vs C/N plots, with 367-GC sediment samples showing the lowest $\delta^{15}N_d$ values and lowest C/N ratios (Figs. 4b, c). The models suggests that the most ^{13}C-depleted sample (−42.0‰) comprises 45.2% MOM, 5.7% TOM, and 49.1% ANME-SRB biomass. The latter value is higher than the amounts of AOM-derived carbon found in two seep locations in the South China Sea, showing AOM contributions up to 6.4% of the total sedimentary organic carbon (cf. Li et al., 2023). The uncertainty related to our selected end-member $\delta^{13}C_{org}$ value for ANME-SRB cannot explain this difference, since a $\delta^{13}C_{org} = -120.0‰$ would result in a contribution of 40.5%. Therefore, it is likely that the high value in our study is due to the longer stability of the SMTZ at this stratigraphic interval in core 367-GC and/or relatively low marine productivity (Li et al., 2023). The amount of carbon and nitrogen derived from ANME-SRB biomass in that sample corresponds to 0.27% (TOC = 0.56%) and 0.030% (TN_d = 0.061%), respectively. We attempted to provide a time constraint for AOM activity by assuming (1) all nitrogen in ANME-SRB biomass derives from nitrogen fixation, (2) a constant nitrogen fixation rate of 114 pmol N_2 g_{dw} h^{-1} for ANME-SRB consortia (Dekas et al., 2018), (3) continuous supply of dinitrogen via diffusion, (4) negligible diagenetic nitrogen loss, and (5) a gram of dry sediment contains 0.00218 mol nitrogen (0.061 wt%). Based on these assumptions, it would take approximately 2183 years to produce the observed geochemical anomaly. We are aware that this estimate is affected by significant uncertainties, but it provides a tentative first-order estimation of the duration of AOM, which is consistent with the precipitation of cm-sized MDAC concretions (Luff et al., 2004) and barite front formation (Feng et al., 2019) observed in the same stratigraphic interval. The rate of nitrogen incorporation via ammonium assimilation is three orders of magnitude higher than for diazotrophy (Siegert et al., 2013), and would yield values inconsistent with the time constraints imposed by the other geochemical proxies for AOM in the same interval. In seep-impacted sediments off the western coast of the United States, diazotrophy accounted for up to 30% of the total nitrogen requirement in ex-situ experiments, with the remaining fraction provided by ammonium assimilation (Dekas et al., 2018). In this study, no pore fluid nitrogen species (NO_3, NH_4^+, N_2) were measured, hampering any quantification of nitrogen fluxes in the SMTZ. Although it remains unclear which source dominated the uptake of inorganic nitrogen in the investigated gas-hydrate bearing sediment, the stable isotopic signals ($\delta^{13}C_{org}$, $\delta^{15}N_d$) associated with methane-derived carbonates provided clear in-situ evidence for significant nitrogen assimilation.

4.3. Rethinking the role of methane seeps in the global nitrogen cycle

The relative balance between nitrogen sources, i.e. nitrogen fixation, and losses via denitrification, anaerobic ammonium oxidation (anammox), and sediment burial regulates the long-term oceanic nitrogen budget, directly affecting marine productivity and Earth's climate (Altabet, 2007; Gruber and Galloway, 2008). The sedimentary nitrogen isotope composition ($\delta^{15}N$) of organic matter has been widely used to reconstruct the past marine nitrogen cycle over centennial to geological time scales (Gruber and Galloway, 2008). The application of this proxy mainly relies on the large isotopic fractionation associated with water column denitrification (ε ~20–30‰) as opposed to the negligible effect for sedimentary denitrification and nitrogen fixation (Sigman and Casciotti, 2001), with the average oceanic $\delta^{15}N$ signature controlled by the former process under steady-state conditions. Geological periods marked by high denitrification rates, recorded in the sedimentary record of organic nitrogen ($\delta^{15}N$), correspond to peaks in atmospheric carbon dioxide, suggesting a potential contribution of denitrification to past climate change over glacial-interglacial periods (Altabet, 2007; Gruber and Galloway, 2008). Today's oceanic nitrogen budget seems to be imbalanced, with deficit estimates ranging from −183 to −62 Tg N y^{-1} (Codispoti et al., 2001). However, there are still large uncertainties on fluxes associated with sources and sinks, hindering a profound understanding of nitrogen cycling and predictions of future responses to anthropogenic perturbations (Altabet, 2007; Gruber and Galloway,

2008).

Nitrogen cycling at methane seeps remains largely unconstrained. Here, we showed that the light $\delta^{15}N$ composition of bulk decarbonated sediments in combination with low $\delta^{13}C_{org}$ values can be used as a proxy for AOM-driven nitrogen assimilation. Such a pattern was recognized in a sediment interval directly overlying a gas hydrate-rich layer, suggesting that high intensity and longevity of methane oxidation are prerequisites for a detectable accumulation of ^{15}N-depleted ANME-SRB biomass, in line with experimental observations (Dekas et al., 2014). Our interpretation is not only supported by experimental evidence for the capacity of AOM consortia to incorporate nitrogen (Dekas et al., 2016; Dekas et al., 2009; Metcalfe et al., 2021; Miyazaki et al., 2009; Orphan et al., 2009; Pernthaler et al., 2008), but also by incubation studies on seep sediments collected from Mound 12 mud volcano offshore Costa Rica reporting narrow peaks in nitrogen fixation rates at sediment depths corresponding to an increased abundance of AOM consortia (Dekas et al., 2014). Therefore, the new evidence for this process from the environment validates the relevance of ex-situ microbiological investigations and carries important biogeochemical implications. First, this discovery expands the distribution of marine nitrogen uptake to the sedimentary subsurface. It confirms the need for more accurate quantification of the nitrogen sinks in seep-impacted sediments (Dekas et al., 2014). Second, the new findings confirm the efficiency of a comprehensive geochemical approach to explore AOM-related nitrogen cycle in sediments and the geological record. The large $\delta^{15}N$ offset of −4.2 ‰ observed in gas-hydrate bearing sediment of Håkon Mosby Mud Volcano resembles negative excursions of up to −5 ‰ in sediments from the Haima seeps of the South China Sea (Hu et al., 2020), which were interpreted as evidence of AOM-driven nitrogen uptake. Methane seeps and gas hydrate-bearing sediments are widespread along continental margins (Piñero et al., 2013) and may represent a hitherto unaccounted key element of the marine nitrogen cycle. Future larger-scale investigations in gas hydrate-bearing regions will be critical to quantify nitrogen fluxes, eventually closing the gap in global deep-sea nitrogen budgets. Such studies shall include the characterization of the nitrogen geochemistry of pore fluids as well as the application of compound-specific nitrogen isotope analysis of amino acids (Ohkouchi et al., 2017) for the development of fine-tuned nitrogen isotope-based biogeochemical proxies of AOM-driven diazotrophy and ammonium assimilation in modern and ancient marine sediments.

5. Conclusions

Methanotrophic communities inhabiting seep environments are able to assimilate and share inorganic nitrogen, but definitive geochemical evidence under in-situ conditions is still missing, limiting our understanding of nitrogen cycling in these peculiar environments and of their contribution to the global nitrogen cycle.

Here we report evidence from hydrate-bearing sediments for nitrogen uptake based on sediment and pore fluid geochemistry of two gravity cores collected from Håkon Mosby Mud Volcano, SW Barents Sea. Gravity core 367-GC intercepted a shallow gas hydrate layer at 67 cm below the seafloor, whereas core 369-GC was collected in a background area 16 km away from the outer volcanic rim not affected by seepage. XRF data of core 367-GC indicated the presence of a carbonate-rich interval above the gas hydrate layer. The isotopic composition ($\delta^{13}C$, $\delta^{18}O$) of two small carbonate concretions isolated from that interval yielded $\delta^{13}C$ values of −31.8‰ and − 31.6‰, and $\delta^{18}O$ values of 6.1‰ and 5.8‰, indicating the incorporation of methane-derived carbon and isotopically heavy oxygen released from the underlying gas hydrate. Today's sulfate-methane transition is located ~30 cm above this interval, reflecting a recent increase in methane flux from the underlying gas hydrate layer. The carbonate-rich interval strikingly matches with low $\delta^{13}C$ values of organic matter, as low as −42.0 ‰, and low $\delta^{15}N$ values of the bulk decarbonated sediment (1.2 ‰). Using stable isotope mixing models including marine, terrestrial, and AOM-derived biomass end-member compositions, we demonstrate the uptake of inorganic nitrogen in association with AOM in two stratigraphic intervals corresponding to paleo sulfate-methane transition zones in the hydrate bearing core. AOM-derived biomass contributes to up to 49.1 wt % of the bulk sediment organic matter. The comprehensive isotopic approach presented in this study can be used to explore the AOM-related nitrogen cycle in both modern settings and the geological record. Overall, this discovery calls for a reassessment of the role of methane seeps in the marine nitrogen cycle and emphasizes the importance of conducting more extensive studies in regions with gas hydrates to better understand the nitrogen sources and fluxes in the sediment, ultimately leading to a more comprehensive understanding of deep-sea nitrogen budgets.

Author contributions

CA and GP conceptualized the study. CA conducted the samplings, wrote the initial manuscript and generated the figs. CW carried out the sediment sample preparation and analyses. CA, CW, JP and GP all contributed to the interpretation of the datasets and to the improvement of the manuscript.

Declaration of Competing Interest

The authors declare no competing interests.

Data availability

All data used for this study are included in the manuscript and in the supplementary materal.

Acknowledgments

The research was funded by the AKMA project (RCN grant No. 287869) within the frame of the Centre for Arctic Gas Hydrate, Environment and Climate (CAGE) (RCN grant No. 223259). We acknowledge the captain, chief scientists Kate Waghorn and Malin Waage, and crew onboard R/V Helmer Hanssen for their assistance during the expedition CAGE20-3. We are grateful to Matteus Lindgren (SIL-UiT) for technical support in stable isotope analysis and the laboratory staff of the Department of Geosciences (UiT) for support during core logging. We thank two anonymous reviewers for comments and suggestions that improved the manuscript.

Appendix A. Supplementary data

Supplementary data to this article can be found online at https://doi.org/10.1016/j.chemgeo.2023.121638.

References

Altabet, M.A., 2005. Isotopic Tracers of the Marine Nitrogen Cycle : Present and Past, 2, pp. 1–43.

Altabet, M.A., 2007. Constraints on oceanic N balance/imbalance from sedimentary15N records. Biogeosciences 4, 75–86. https://doi.org/10.5194/bg-4-75-2007.

Argentino, C., Waghorn, K.A., Vadakkepuliyambatta, S., Polteau, S., Bünz, S., Panieri, G., 2021. Dynamic and history of methane seepage in the SW Barents Sea: new insights from Leirdjupet Fault complex. Sci. Rep. 11, 4373. https://doi.org/10.1038/s41598-021-83542-0.

Argentino, C., Savini, A., Panieri, G., 2022. Integrating Fine-Scale Habitat Mapping and Pore Water Analysis in Cold Seep Research: A Case Study from the SW Barents Sea. In: World Atlas of Submarine Gas Hydrates in Continental Margins. Springer International Publishing, Cham, pp. 505–514. https://doi.org/10.1007/978-3-030-81186-0_43.

Bertics, V., Sohm, J., Treude, T., Chow, C., Capone, D., Fuhrman, J., Ziebis, W., 2010. Burrowing deeper into benthic nitrogen cycling: the impact of bioturbation on nitrogen fixation coupled to sulfate reduction. Mar. Ecol. Prog. Ser. 409, 1–15. https://doi.org/10.3354/meps08639.

Boetius, A., Ravenschlag, K., Schubert, C.J., Rickert, D., Widdel, F., Gieseke, A., Amann, R., Jørgensen, B.B., Witte, U., Pfannkuche, O., Gleseke, A., Amann, R.,

Jørgensen, B.B., Witte, U., Pfannkuche, O., 2000. A marine microbial consortium apparently mediating anaerobic oxidation of methane. Nature 407, 623–626. https://doi.org/10.1038/35036572.
Bünz, S., Panieri, G., 2022. CAGE21-1 Cruise Report: AKMA-AKER-GReAT. CAGE – Cent. Arct. Gas Hydrate, Environ. Clim. Rep. Ser. 9 https://doi.org/10.7557/cage.6677.
Codispoti, L.A., 2007. An oceanic fixed nitrogen sink exceeding 400 Tg N a−1 vs the concept of homeostasis in the fixed-nitrogen inventory. Biogeosciences 4, 233–253. https://doi.org/10.5194/bg-4-233-2007.
Codispoti, L.A., Brandes, J.A., Christensen, J.P., Devol, A.H., Naqvi, S.W.A., Paerl, H.W., Yoshinari, T., 2001. The oceanic fixed nitrogen and nitrous oxide budgets: moving targets as we enter the anthropocene? Sci. Mar. 65, 85–105. https://doi.org/10.3989/scimar.2001.65s285.
Crameri, F., Shephard, G.E., Heron, P.J., 2020. The misuse of colour in science communication. Nat. Commun. 11, 1–10. https://doi.org/10.1038/s41467-020-19160-7.
Davidson, D.W., Leaist, D.G., Hesse, R., 1983. Oxygen-18 enrichment in the water of a clathrate hydrate. Geochim. Cosmochim. Acta 47, 2293–2295. https://doi.org/10.1016/0016-7037(83)90053-4.
Dekas, A.E., Poretsky, R.S., Orphan, V.J., 2009. Deep-sea archaea fix and share nitrogen in methane-consuming microbial consortia. Science 80 (326), 422–426. https://doi.org/10.1126/science.1178223.
Dekas, A.E., Chadwick, G.L., Bowles, M.W., Joye, S.B., Orphan, V.J., 2014. Spatial distribution of nitrogen fixation in methane seep sediment and the role of the ANME archaea. Environ. Microbiol. 16, 3012–3029. https://doi.org/10.1111/1462-2920.12247.
Dekas, A.E., Connon, S.A., Chadwick, G.L., Trembath-Reichert, E., Orphan, V.J., 2016. Activity and interactions of methane seep microorganisms assessed by parallel transcription and FISH-NanoSIMS analyses. ISME J. 10, 678–692. https://doi.org/10.1038/ismej.2015.145.
Dekas, A.E., Fike, D.A., Chadwick, G.L., Green-Saxena, A., Fortney, J., Connon, S.A., Dawson, K.S., Orphan, V.J., 2018. Widespread nitrogen fixation in sediments from diverse deep-sea sites of elevated carbon loading. Environ. Microbiol. 20, 4281–4296. https://doi.org/10.1111/1462-2920.14342.
Dong, X., Zhang, C., Peng, Y., Zhang, H.-X., Shi, L.-D., Wei, G., Hubert, C.R.J., Wang, Y., Greening, C., 2022. Phylogenetically and catabolically diverse diazotrophs reside in deep-sea cold seep sediments. Nat. Commun. 13, 4885. https://doi.org/10.1038/s41467-022-32503-w.
Egger, M., Riedinger, N., Mogollón, J.M., Jørgensen, B.B., 2018. Global diffusive fluxes of methane in marine sediments. Nat. Geosci. 11, 421–425. https://doi.org/10.1038/s41561-018-0122-8.
Eigenbrode, J.L., Freeman, K.H., 2006. Late Archean rise of aerobic microbial ecosystems. Proc. Natl. Acad. Sci. 103, 15759–15764. https://doi.org/10.1073/pnas.0607540103.
Elvert, M., Hopmans, E.C., Treude, T., Boetius, A., Suess, E., 2005. Spatial variations of methanotrophic consortia at cold methane seeps: Implications from a high-resolution molecular and isotopic approach. Geobiology 3, 195–209. https://doi.org/10.1111/j.1472-4669.2005.00051.x.
Emerson, S., Hedges, J.I., 1988. Processes controlling the organic carbon content of open ocean sediments. Paleoceanography 3, 621–634. https://doi.org/10.1029/PA003i005p00621.
Faleide, J.I., Solheim, A., Fiedler, A., Hjelstuen, B.O., Andersen, E.S., Vanneste, K., 1996. Late Cenozoic evolution of the western Barents Sea-Svalbard continental margin. Glob. Planet. Chang. 12, 53–74. https://doi.org/10.1016/0921-8181(95)00012-7.
Feng, J., Yang, S., Wang, H., Liang, J., Fang, Y., Luo, M., 2019. Methane source and turnover in the shallow sediments to the west of Haima cold seeps on the northwestern slope of the South China Sea. Geofluids 2019, 1–18. https://doi.org/10.1155/2019/1010824.
Feng, D., Pohlman, J.W., Peckmann, J., Sun, Y., Hu, Y., Roberts, H.H., Chen, D., 2021. Contribution of deep-sourced carbon from hydrocarbon seeps to sedimentary organic carbon: evidence from radiocarbon and stable isotope geochemistry. Chem. Geol. 585 https://doi.org/10.1016/j.chemgeo.2021.120572.
Fischer, D., Sahling, H., Nöthen, K., Bohrmann, G., Zabel, M., Kasten, S., 2012. Interaction between hydrocarbon seepage, chemosynthetic communities, and bottom water redox at cold seeps of the Makran accretionary prism: Insights from habitat-specific pore water sampling and modeling. Biogeosciences 9, 2013–2031. https://doi.org/10.5194/bg-9-2013-2012.
Friedman, I., O'Neil, J.R., 1986. Compilation of Stable Isotope Fractionation Factors of Geochemical Interest. In: Data of Geochemistry.
Fulweiler, R.W., 2009. Fantastic Fixers. Science 80 (326), 377–378. https://doi.org/10.1126/science.1181129.
Gruber, N., Galloway, J.N., 2008. An Earth-system perspective of the global nitrogen cycle. Nature 451, 293–296. https://doi.org/10.1038/nature06592.
Hachikubo, A., Kosaka, T., Kida, M., Krylov, A., Sakagami, H., Minami, H., Takahashi, N., Shoji, H., 2007. Isotopic fractionation of methane and ethane hydrates between gas and hydrate phases. Geophys. Res. Lett. 34, 1–5. https://doi.org/10.1029/2007GL030557.
Hinrichs, K.-U., Summons, R.E., Orphan, V., Sylva, S.P., Hayes, J.M., 2000. Molecular and isotopic analysis of anaerobic methane-oxidizing communities in marine sediments. Org. Geochem. 31, 1685–1701. https://doi.org/10.1016/S0146-6380(00)00106-6.
Hjelstuen, B.O., Eldholm, O., Faleide, J.I., Vogt, P.R., 1999. Regional setting of Håkon Mosby Mud Volcano, SW Barents Sea margin. Geo-Marine Lett. 19, 22–28. https://doi.org/10.1007/s003670050089.
Hoch, M.P., Fogel, M.L., Kirchman, D.L., 1992. Isotope fractionation associated with ammonium uptake by a marine bacterium. Limnol. Oceanogr. 37, 1447–1459. https://doi.org/10.4319/lo.1992.37.7.1447.
House, C.H., Orphan, V.J., Turk, K.A., Thomas, B., Pernthaler, A., Vrentas, J.M., Joye, S. B., 2009. Extensive carbon isotopic heterogeneity among methane seep microbiota, 11, 2207–2215. https://doi.org/10.1111/j.1462-2920.2009.01934.x.
Hu, Y., Feng, D., Peng, Y., Peckmann, J., Kasten, S., Wang, X., Liang, Q., Wang, H., Chen, D., 2020. A prominent isotopic fingerprint of nitrogen uptake by anaerobic methanotrophic archaea. Chem. Geol. 558, 119972 https://doi.org/10.1016/j.chemgeo.2020.119972.
Hutchins, D.A., Capone, D.G., 2022. The marine nitrogen cycle: new developments and global change. Nat. Rev. Microbiol. 20, 401–414. https://doi.org/10.1038/s41579-022-00687-z.
Joye, S.B., Boetius, A., Orcutt, B.N., Montoya, J.P., Schulz, H.N., Erickson, M.J., Lugo, S. K., 2004. The anaerobic oxidation of methane and sulfate reduction in sediments from Gulf of Mexico cold seeps. Chem. Geol. 205, 219–238. https://doi.org/10.1016/j.chemgeo.2003.12.019.
Kasten, S., Zabel, M., Heuer, V., Hensen, C., 2003. Processes and Signals of Nonsteady-State Diagenesis in Deep-Sea Sediments and their Pore Waters. In: The South Atlantic in the Late Quaternary. https://doi.org/10.1007/978-3-642-18917-3_20.
Kienast, M., Higginson, M.J., Mollenhauer, G., Eglinton, T.I., Chen, M.-T., Calvert, S.E., 2005. On the sedimentological origin of down-core variations of bulk sedimentary nitrogen isotope ratios. Paleoceanography 20, n/a-n/a. https://doi.org/10.1029/2004PA001081.
Kim, S., Neil, J.R.O., Hillaire-marcel, C., Mucci, A., 2007. Oxygen Isotope Fractionation between Synthetic Aragonite and Water : Influence of Temperature and Mg2 + Concentration oxygen Isotope Fractionation between Synthetic Aragonite and Water : Influence of Temperature and mg 2 + Concentration. https://doi.org/10.1016/j.gca.2007.04.019.
Knies, J., Martinez, P., 2009. Organic matter sedimentation in the western Barents Sea region: Terrestrial and marine contribution based on isotopic composition and organic nitrogen content. Nor. Geol. Tidsskr. 89, 79–89.
Knies, J., Brookes, S., Schubert, C.J., 2007. Re-assessing the nitrogen signal in continental margin sediments: New insights from the high northern latitudes. Earth Planet. Sci. Lett. 253, 471–484. https://doi.org/10.1016/j.epsl.2006.11.008.
Knittel, K., Lösekann, T., Boetius, A., Kort, R., Amann, R., 2005. Diversity and distribution of Methanotrophic Archaea at Cold Seeps. Appl. Environ. Microbiol. 71, 467–479. https://doi.org/10.1128/AEM.71.1.467-479.2005.
Lee, D.-H., Kim, J.-H., Lee, Y.M., Stadnitskaia, A., Jin, Y.K., Niemann, H., Kim, Y.-G., Shin, K.-H., 2018. Biogeochemical evidence of anaerobic methane oxidation on active submarine mud volcanoes on the continental slope of the Canadian Beaufort Sea. Biogeosciences 15, 7419–7433. https://doi.org/10.5194/bg-15-7419-2018.
Lee, D.H., Lee, Y.M., Kim, Jung Hyun, Jin, Y.K., Paull, C., Niemann, H., Kim, Ji Hoon, Shin, K.H., 2019. Discriminative biogeochemical signatures of methanotrophs in different chemosynthetic habitats at an active mud volcano in the Canadian Beaufort Sea. Sci. Rep. 9, 1–13. https://doi.org/10.1038/s41598-019-53950-4.
Lehmann, M.F., 2002. Preservation of Organic Matter and Alteration of its Carbon and Nitrogen Isotope Composition During Simulated and In Situ Early Sedimentary Diagenesis Preservation of Organic Matter and Alteration of its Carbon and Nitrogen Isotope Composition During Simulated and In Situ Early Sedimentary Diagenesis. https://doi.org/10.1016/S0016-7037(02)00968-7.
Lein, A., Vogt, P., Crane, K., Egorov, A., Ivanov, M., 1999. Chemical and isotopic evidence for the nature of the fluid in CH 4 -containing sediments of the Håkon Mosby Mud Volcano. Geo-Marine Lett. 19, 76–83. https://doi.org/10.1007/s003670050095.
Li, Y., Xu, X., Pang, L., Guan, P., Fang, Y., Lu, H., Ye, J., Xie, W., 2022. Elemental and Isotopic Signatures of Bulk Sedimentary Organic Matter in Shenhu Area, Northern South China Sea. Front. Earth Sci. 10, 1–15. https://doi.org/10.3389/feart.2022.836381.
Li, N., Meng, J., Peckmann, J., Chen, D., Feng, D., 2023. Quantification of the sources of sedimentary organic carbon at methane seeps : a case study from the South China Sea. Chem. Geol. 627, 121463 https://doi.org/10.1016/j.chemgeo.2023.121463.
Luff, R., Wallmann, K., Aloisi, G., 2004. Numerical modeling of carbonate crust formation at cold vent sites: significance for fluid and methane budgets and chemosynthetic biological communities. Earth Planet. Sci. Lett. 221, 337–353. https://doi.org/10.1016/S0012-821X(04)00107-4.
Madigan, M.T., Bender, K.S., Buckley, D.H., Sattley, M.W., Stahl, D.A., 2017. Brock Biology of Microorganisms, Global Edition, 15th Editi. ed. Pearson Education Limited.
Mahaffey, C., 2005. The conundrum of marine N2 fixation. Am. J. Sci. 305, 546–595. https://doi.org/10.2475/ajs.305.6-8.546.
Marlow, J.J., Steele, J.A., Ziebis, W., Thurber, A.R., Levin, L.A., Orphan, V.J., 2014. Carbonate-hosted methanotrophy represents an unrecognized methane sink in the deep sea. Nat. Commun. 5 https://doi.org/10.1038/ncomms6094.
McGlynn, S.E., Chadwick, G.L., Kempes, C.P., Orphan, V.J., 2015. Single cell activity reveals direct electron transfer in methanotrophic consortia. Nature 526, 531–535. https://doi.org/10.1038/nature15512.
Metcalfe, K.S., Murali, R., Mullin, S.W., Connon, S.A., Orphan, V.J., 2021. Experimentally-validated correlation analysis reveals new anaerobic methane oxidation partnerships with consortium-level heterogeneity in diazotrophy. ISME J. 15, 377–396. https://doi.org/10.1038/s41396-020-00757-1.
Meyers, P.A., 1994. Preservation of elemental and isotopic source identification of sedimentary organic matter. Chem. Geol. 114, 289–302. https://doi.org/10.1016/0009-2541(94)90059-0.
Meyers, P.A., 1997. Organic geochemical proxies of paleoceanographic, paleolimnologic, and paleoclimatic processes. Org. Geochem. 27, 213–250. https://doi.org/10.1016/S0146-6380(97)00049-1.
Miao, X., Feng, X., Hu, L., Li, J., Liu, X., Wang, N., Xiao, Q., Wei, J., 2022. Coupled $\delta^{15}N_{TN}$ and $\delta^{13}C_{TOC}$ Insights into methane Seepage Activities in Bulk Marine

Sediments of the Qiongdongnan Basin, South China Sea. J. Ocean Univ. China 21, 1495–1503. https://doi.org/10.1007/s11802-022-5049-4.
Milkov, A.V., Vogt, P.R., Crane, K., Lein, A.Y., Sassen, R., Cherkashev, G.A., 2004. Geological, geochemical, and microbial processes at the hydrate-bearing Håkon Mosby mud volcano: a review. Chem. Geol. 205, 347–366. https://doi.org/10.1016/j.chemgeo.2003.12.030.
Miyazaki, J., Higa, R., Toki, T., Ashi, J., Tsunogai, U., Nunoura, T., Imachi, H., Takai, K., 2009. Molecular characterization of potential nitrogen fixation by anaerobic methane-oxidizing archaea in the methane seep sediments at the number 8 Kumano Knoll in the Kumano Basin, offshore of Japan. Appl. Environ. Microbiol. 75, 7153–7162. https://doi.org/10.1128/AEM.01184-09.
Montoya, J.P., 2008. Nitrogen Stable Isotopes in Marine Environments. Nitrogen Mar. Environ. 1277–1302 https://doi.org/10.1016/B978-0-12-372522-6.00029-3.
Niemann, H., Lösekann, T., de Beer, D., Elvert, M., Nadalig, T., Knittel, K., Amann, R., Sauter, E.J., Schlüter, M., Klages, M., Foucher, J.P., Boetius, A., 2006. Novel microbial communities of the Haakon Mosby mud volcano and their role as a methane sink. Nature 443, 854–858. https://doi.org/10.1038/nature05227.
Ohkouchi, N., Chikaraishi, Y., Close, H.G., Fry, B., Larsen, T., Madigan, D.J., McCarthy, M.D., McMahon, K.W., Nagata, T., Naito, Y.I., Ogawa, N.O., Popp, B.N., Steffan, S., Takano, Y., Tayasu, I., Wyatt, A.S.J., Yamaguchi, Y.T., Yokoyama, Y., 2017. Advances in the application of amino acid nitrogen isotopic analysis in ecological and biogeochemical studies. Org. Geochem. 113, 150–174. https://doi.org/10.1016/j.orggeochem.2017.07.009.
Orphan, V.J., Hinrichs, K.-U., Ussler, W., Paull, C.K., Taylor, L.T., Sylva, S.P., Hayes, J. M., Delong, E.F., 2001. Comparative analysis of methane-oxidizing archaea and sulfate-reducing bacteria in anoxic marine sediments. Appl. Environ. Microbiol. 67, 1922–1934. https://doi.org/10.1128/AEM.67.4.1922-1934.2001.
Orphan, V.J., Turk, K.A., Green, A.M., House, C.H., 2009. Patterns of ^{15}N assimilation and growth of methanotrophic ANME-2 archaea and sulfate-reducing bacteria within structured syntrophic consortia revealed by FISH-SIMS. Environ. Microbiol. 11, 1777–1791. https://doi.org/10.1111/j.1462-2920.2009.01903.x.
Pape, T., Feseker, T., Kasten, S., Fischer, D., Bohrmann, G., 2011. Distribution and abundance of gas hydrates in near-surface deposits of the Håkon Mosby Mud Volcano, SW Barents Sea. Geochem. Geophys. Geosyst. 12 https://doi.org/10.1029/2011GC003575.
Perez-Garcia, C., Feseker, T., Mienert, J., Berndt, C., 2009. The Håkon Mosby mud volcano: 330 000 years of focused fluid flow activity at the SW Barents Sea slope. Mar. Geol. 262, 105–115. https://doi.org/10.1016/j.margeo.2009.03.022.
Pernthaler, A., Dekas, A.E., Brown, C.T., Goffredi, S.K., Embaye, T., Orphan, V.J., 2008. Diverse syntrophic partnerships from deep-sea methane vents revealed by direct cell capture and metagenomics. Proc. Natl. Acad. Sci. 105, 7052–7057. https://doi.org/10.1073/pnas.0711303105.
Piñero, E., Marquardt, M., Hensen, C., Haeckel, M., Wallmann, K., 2013. Estimation of the global inventory of methane hydrates in marine sediments using transfer functions. Biogeosciences 10, 959–975. https://doi.org/10.5194/bg-10-959-2013.
Pohlman, J.W., Riedel, M., Bauer, J.E., Canuel, E.A., Paull, C.K., Lapham, L., Grabowski, K.S., Coffin, R.B., Spence, G.D., 2013. Anaerobic methane oxidation in low-organic content methane seep sediments. Geochim. Cosmochim. Acta 108, 184–201. https://doi.org/10.1016/j.gca.2013.01.022.
Reeburgh, W.S., 2007. Oceanic methane Biogeochemistry. Chem. Rev. 107, 486–513. https://doi.org/10.1021/cr050362v.
Riedinger, N., Kasten, S., Gröger, J., Franke, C., Pfeifer, K., 2006. Active and buried authigenic barite fronts in sediments from the Eastern Cape Basin. Earth Planet. Sci. Lett. 241, 876–887. https://doi.org/10.1016/j.epsl.2005.10.032.
Schreiber, L., Holler, T., Knittel, K., Meyerdierks, A., Amann, R., 2010. Identification of the dominant sulfate-reducing bacterial partner of anaerobic methanotrophs of the ANME-2 clade. Environ. Microbiol. https://doi.org/10.1111/j.1462-2920.2010.02275.x no-no.
Schulz, H.D., 2006. Quantification of early Diagenesis : Dissolved Constituents in Pore Water and Signals in the Solid phase. In: Marine Geochemistry. Springer, Berlin, Heidelberg, pp. 73–124.
Siegert, M., Taubert, M., Seifert, J., von Bergen-Tomm, M., Basen, M., Bastida, F., Gehre, M., Richnow, H.-H., Krüger, M., 2013. The nitrogen cycle in anaerobic methanotrophic mats of the Black Sea is linked to sulfate reduction and biomass decomposition. FEMS Microbiol. Ecol. 86, 231–245. https://doi.org/10.1111/1574-6941.12156.
Sigman, D.M., Casciotti, K.L., 2001. Nitrogen Isotopes in the Ocean. In: Encyclopedia of Ocean Sciences. Elsevier, pp. 1884–1894. https://doi.org/10.1006/rwos.2001.0172.
Wada, E., 1980. Nitrogen isotope fractionation and its significance in biogeochemical processes occurring in marine environments. Isot. Mar. Chem. 375–398.
Weber, T., Wiseman, N.A., Kock, A., 2019. Global Ocean methane emissions dominated by shallow coastal waters. Nat. Commun. 10, 1–10. https://doi.org/10.1038/s41467-019-12541-7.
Wegener, G., Krukenberg, V., Riedel, D., Tegetmeyer, H.E., Boetius, A., 2015. Intercellular wiring enables electron transfer between methanotrophic archaea and bacteria. Nature 526, 587–590. https://doi.org/10.1038/nature15733.
Whiticar, M.J., 1999. Carbon and hydrogen isotope systematics of bacterial formation and oxidation of methane. Chem. Geol. 161, 291–314. https://doi.org/10.1016/S0009-2541(99)00092-3.
Xiong, P., Lu, H., Xie, X., Zhang, G., Fu, S., Jiang, L., Zhang, P., 2020. Geochemical responses and implications for gas hydrate accumulation: Case study from site SHC in Shenhu Area within northern South China Sea. Mar. Pet. Geol. 111, 650–661. https://doi.org/10.1016/j.marpetgeo.2019.06.032.
Yamanaka, T., Shimamura, S., Chikaraishi, Y., Haga, T., Fujiwara, Y., 2015. Re-evaluation of nutrient sources for deep-sea wood-boring bivalves using the isotopic composition of bulk C, N, S, and amino acid nitrogen. Mar. Ecol. Prog. Ser. 540, 157–165. https://doi.org/10.3354/meps11510.
Yoshinaga, M.Y., Lazar, C.S., Elvert, M., Lin, Y., Zhu, C., Heuer, V.B., Teske, A., Hinrichs, K., 2015. Possible roles of uncultured archaea in carbon cycling in methane-seep sediments, 164, 35–52.
Zhang, X., Sigman, D.M., Morel, F.M.M., Kraepiel, A.M.L., 2014. Nitrogen isotope fractionation by alternative nitrogenases and past ocean anoxia. Proc. Natl. Acad. Sci. 111, 4782–4787. https://doi.org/10.1073/pnas.1402976111.